A Quantitative Study of the in Vitro Binding of the C-Terminal Domain of p21 to PCNA: Affinity, Stoichiometry, and Thermodynamics

Daniella I. Zheleva,*,‡ Nikolai Z. Zhelev,‡ Peter M. Fischer,‡ Susan V. Duff,‡ Emma Warbrick,§ David G. Blake,‡ and David P. Lane§

Dundee Technopole, Cyclacel Ltd., James Lindsay Place, Dundee DD1 5JJ, U.K., and CRC Laboratories, Department of Biochemistry, University of Dundee, Dundee DD1 4HN, U.K.

Received October 28, 1999; Revised Manuscript Received April 18, 2000

ABSTRACT: Proliferating cell nuclear antigen (PCNA) plays an essential role in DNA replication, repair, and control of cell proliferation, and its activity can be modulated by interaction with $p21^{Waf1/Cip1}$ [Cox, L. S., (1997) *Trends Cell Biol. 7*, 493−497]. This protein−protein interaction provides a particularly good model target for designing therapeutic agents to treat proliferative disorders such as cancer. In this study, the formation of complexes between PCNA and peptides derived from the C-terminus of p21 has been investigated at the molecular level and quantified using a competitive PCNA binding assay and isothermal titration calorimetry (ITC). The affinity constant for the interaction between p21 (141−160) peptide and PCNA has been determined to be 1.14×10^7 M^{-1}, corresponding to a K_d of 87.7 nM. Measurement of the interaction of truncation and substitution analogues based on the p21 (141−160) sequence with PCNA revealed that the N-terminal part (residues 141−152) of the above peptide is the minimum recognition motif, required for PCNA binding. Truncation of the C-terminal region p21 (153−160), though, inhibited significantly the ability of the peptides to compete with the full-length p21 (141−160) for binding to PCNA. Alanine mutation of Met 147 or Asp 149 completely abolished or significantly decreased, respectively, the level of the PCNA binding and the inhibition of SV40 DNA replication. Comparison of the data obtained by the competitive PCNA binding assay and the ITC measurements demonstrated the usefulness of this assay for screening for compounds that could modulate the PCNA−p21 interaction. Using this assay, we have screened rationally designed peptides for binding to PCNA and interruption of the PCNA−p21 (141−160) complex. As a result of this screening, we have identified a 16-residue peptide (consensus motif 1 peptide) with the following sequence: SAVLQKKITDYFHPKK. Consensus motif 1 peptide and p21 (141−160) have similar affinities for binding PCNA and abilities to inhibit in vitro replication of DNA originated from SV40. Such peptides could prove useful in assessing p21-mimetic strategies for cancer treatment.

Proliferating cell nuclear antigen (PCNA)[1] is an essential protein found in all proliferating eukaryotic cells, and carries out crucial roles in both DNA replication and DNA repair (*1*, *2*). The protein has a trimeric ring structure that might slide along duplex DNA and form a platform for association with a variety of proteins, in particular, holding the DNA polymerases in close association with their template (*3*, *4*).

Trimeric PCNA is loaded onto duplex DNA by the action of a multisubunit replication protein, RFC, using energy from ATP hydrolysis (*5*). PCNA is involved in synthesis of both leading and lagging DNA strands, providing an anchorage site and increasing the processivity of DNA pol δ (*6*, *7*) and DNA pol ϵ (*8*), respectively. In addition, PCNA interacts with and stimulates Flap endonuclease 1 (Fen 1) which is required for Okazaki fragment processing (*9*). PCNA is required for nucleotide excision repair (*10*) and mismatch repair (*11*).

A role for PCNA in the cell cycle control is recognized on the basis of the interaction with cyclin D (*12*), growth arrest and DNA damage inducible protein Gadd 45 (*13*, *14*), myeloid cell differentation protein MyD 118 (*15*), and the cdk-inhibitor $p21^{Cip1/Waf1/Sdi1}$ protein (reviewed in refs *1*, *2*, and *16*).

p21Cip/Waf1 (hereafter termed p21) is a key mediator of the growth arrest induced by the tumor suppressor protein p53 in response to DNA damage (*17*). p21 acts on CDKs in the G1 and S phases of the cell cycle (reviewed in ref *18*) and also associates with PCNA (*19*). In normal cells, p21 exists in a quaternary complex with a cyclin, a CDK, and PCNA, although the stoichiometry of these complexes is not clear (*17*, *19*−*22*). In transformed cell lines, p21 expression is depressed and CDKs are found in CDK−cyclin binary complexes rather than CDK−cyclin−p21−PCNA quaternary complexes (*17*, *19*, *20*, *22*). p21 contains a PCNA binding motif located in the carboxy-terminal part of the protein between residues 144 and 151 (*23*−*26*). The crystal structure

* To whom correspondence should be addressed. Fax: +44 1382 432155. E-mail: dzheleva@cyclacel.com.

‡ Cyclacel Ltd.

§ University of Dundee.

[1] Abbreviations: CDK, cyclin-dependent kinase; ITC, isothermal titration calorimetry; PAGE, polyacrylamide gel electrophoresis; PBS, phosphate-buffered saline; PCNA, proliferating cell nuclear antigen; pol, polymerase; RFC, replication factor C.

10.1021/bi992498r CCC: $19.00
Published on Web 05/27/2000

of human PCNA complexed with a 22-residue PCNA-binding peptide (PBP) containing this motif has revealed that the p21 carboxy-terminal domain interacts with the interdomain connector loop of PCNA and is likely to prevent the interaction of PCNA with other components of DNA pol assembly (*4*).

p21 has been shown to inhibit PCNA-dependent DNA replication and mismatch repair in vitro (*11*, *27*−*30*) but does not appear to block the function of PCNA in nucleotide excision repair (*28*, *31*, *32*). The mechanism of p21 inhibition of replication has been investigated extensively. RFC-dependent loading of PCNA onto DNA and PCNA-dependent synthesis across single-stranded gaps by DNA pol δ can be blocked by p21 (*29*). Zhang et al. (*33*) showed that DNA pol δ as well as p21 bound to the PCNA interdomain connector loop and their binding sites are overlapping, supporting the view that at least one of the possible mechanisms of inhibition of DNA synthesis by p21 is due to a competition for PCNA binding to DNA pol δ. The amino acid sequences of p21 and Fen 1 are similar, defining the PCNA binding region of each protein (*26*, *34*), and they compete for binding to PCNA (*23*). p21 and p21 PBP have been shown to impair loading of Fen 1 by PCNA on the replication fork in vitro (*23*, *34*), which might contribute to p21 inhibition of replication. In contrast, Fen 1 does not appear to be required for nucleotide excision repair, and inhibition of PCNA−Fen 1 interaction by p21 is therefore unlikely to affect this later process. p21 induction after DNA damage may thus lead to inhibition of cell cycle progression and inactivation of PCNA-dependent DNA replication, while permitting active nucleotide excision repair.

PCNA appears central to many of the molecular switches in the cell that protect genome integrity and control the cell cycle, and p21 is crucial in regulating its activity (*2*). This protein−protein interaction provides a particularly good model target for designing therapeutic agents to treat proliferative disorders such as cancer, and p21-derived agents have already been found to block replication and cell cycle progression in vitro and in cultured cells (*26*, *35*), fueling optimism for rational drug design.

One approach widely used recently for target discovery and rational drug design is mimicking a protein−protein interaction by using a small peptide derived from the full-length protein ligand (*35*−*39*). It has been shown that the biochemical function of mutant p53 could be activated by using small peptides (*40*). The interaction of the oncogene mdm-2 and wild-type p53 could be disrupted through the use of peptidomimetic inhibitors of complex formation (*41*, *42*). Inhibition of CDK4(6)−cyclin D1-induced hypophosphorylation of retinoblastoma protein and cell cycle progression by $p16^{INK4a}$-derived peptides was shown (*39*). The growth suppression function of p21 (*35*, *43*, *44*) could be mimicked by using small peptides derived from the full-length protein (*35*−*37*).

With the aim of defining a small p21-derived peptide which is able to mimic the function of the full-length protein in inhibiting the PCNA activity, we have determined the SAR of a 20-amino acid peptide, derived from the C-terminus of p21 (^{141}KRRQTSMTDFYHSKRRLIFS^{160}), which contains the PCNA binding motif (QTSMTDFY) (*4*, *26*), and characterized the peptide−PCNA interaction by two independent methods: competitive binding of different peptides and immobilized ^{141}KRRQTSMTDFYHSKRRLIFS^{160} to PCNA and isothermal titration calorimetry (ITC). Peptides, containing consensus motifs from different PCNA binding proteins, were designed, and their abilities to mimic the p21−PCNA interaction were tested.

MATERIALS AND METHODS

PCNA Expression. Recombinant human PCNA was expressed in *Escherichia coli* BL21(DE3) from expression vector pT7-PCNA which was a generous gift from B. Stillman. pT7-PCNA contains nucleotides 119−1016 of the human PCNA cDNA (accession number M15796). An *Nde*I site has been introduced at the initiation codon to subclone the PCNA open reading frame as an *Nde*I fragment, placing it under the control of a T7 promoter. The sequence of the PCNA open reading frame was confirmed by automated DNA sequencing. BL21(DE3) pT7-PCNA was grown at 37 °C with shaking (200 rpm) to mid-log phase ($OD_{600} = 0.6$). Expression was induced by the addition of IPTG at a final concentration of 1 mM, and the culture was incubated for a further 3 h (at 37 °C with shaking). The bacteria were then harvested by centrifugation, and the cell pellet was resuspended in 50 mM Tris-HCl (pH 7.5) and 10% sucrose. The resuspended samples were stored at −70 °C until they were required for purification.

PCNA Purification. PCNA was purified by a three-chromatography step procedure. The bacterial pellet (from 2 L of culture) was resuspended in 50 mL of lysis buffer [25 mM Tris-HCl (pH 7.5), 1 mM EDTA, 25 mM NaCl, 0.01% NP-40, 2 mM benzamidine, 1 mM PMSF, and 1 mM DTT]. After sonication (six times, 20 s each), the lysate was clarified by centrifugation for 30 min at 27000*g*. The supernatant was filtered through a 0.45 μm filter (Nalgene) and loaded over a Q Sepharose Fast Flow column (1.6 cm × 15 cm, 30 mL; Pharmacia), pre-equilibrated with 10 column volumes (CV) of Q Sepharose buffer A [25 mM Tris-HCl (pH 7.5), 1 mM EDTA, 0.01% NP-40, 10% glycerol, 2 mM benzamidine, 1 mM PMSF, 1 mM DTT, and 100 mM HaCl] at a flow rate of 1 mL/min. The column was washed with 2 CV of Q Sepharose buffer A, and the bound proteins were eluted with a 10 CV linear salt gradient (100 to 700 mM NaCl in buffer A). Fractions containing PCNA (the protein was eluted with 0.3 M NaCl) were pooled together, and the buffer was exchanged with buffer B [25 mM K_2HPO_4/KH_2PO_4 (pH 7.0), 0.01% NP-40, 10% glycerol, 2 mM benzamidine, 1 mM PMSF, and 1 mM DTT] by ultrafiltration (200 mL stirred ultrafiltration cell and 30 kDa cutoff membrane from Amicon). The sample was loaded over SP Sepharose (1 cm × 12 cm, 10 mL; Pharmacia), pre-equilibrated with 10 CV of buffer B at a flow rate of 1 mL/min. The flowthrough was loaded onto a hydroxyapatite column (1.6 cm × 15 cm, 30 mL; Bio-Rad), pre-equilibrated with 10 CV of buffer B at a flow rate of 0.6 mL/min. The column was washed with 2 CV of buffer B, and the bound proteins were eluted with a 10 CV linear gradient of 25 to 300 mM K_2HPO_4/KH_2PO_4. Fractions containing PCNA were pooled together, concentrated, and buffer exchanged with storage buffer [25 mM Tris-HCl (pH 7.5), 1 mM EDTA, 25 mM NaCl, 0.01% NP-40, 2 mM benzamidine, 1 mM PMSF, 1 mM DTT, and 10% glycerol]. The protein was stored at −70 °C. PCNA fractions were analyzed by SDS−PAGE (*45*); gels were stained with silver.

Size-Exclusion Chromatography. The oligomeric state of PCNA was determined by size-exclusion HPLC. A Superose-12 column (Pharmacia) was used. The mobile phase was 25 mM Tris-HCl (pH 7.5), 2 mM DTT, 200 mM NaCl, and 10% glycerol and the flow rate 0.4 mL/min. The molecular mass was determined using Gel Filtration Chromatography Standard (Bio-Rad): thyroglobulin, 670 000 Da; bovine γ-globulin, 158 000 Da; chiken ovalbumin, 44 000 Da; equine myoglobulin, 17 000 Da; and vitamin B_{12}, 1350 Da.

Labeling of PCNA with Fluorescein. Purified PCNA was labeled with 5(6)-carboxyfluorescein-*N*-hydroxysuccinimide ester (FLUOS) using a Fluorescein Labeling Kit (Boehringer Mannheim Biochemica). FLUOS binds to free amino groups of the protein by forming a stable amide bond. PCNA storage buffer was exchanged with phosphate-buffered saline (PBS) by ultrafiltration (Centricon, 10 kDa cutoff). The final concentration of PCNA was 1 mg/mL. Fifty microliters of FLUOS solution (2 mg/mL in DMSO) was added to 1 mg/mL PCNA. The sample was incubated at room temperature for 2 h with gentle stirring and protected from light. Nonreacted FLUOS was separated on a 9 mL Sephadex G-25 column (Boehringer Mannheim Biochemica). The labeling yield [fluorochrome and protein ratio (*F*/*P*)] was calculated spectrophotometricaly using the following equation:

$$F/P = 3.053(\text{extinction coeff at 495 nm})/[\text{extinction coeff at 280 nm} - 0.255(\text{extinction coeff at 495 nm})]$$

Fluorescein-labeled PCNA was stored at −70 °C.

Peptide Synthesis. Peptides were assembled using a Multipin Peptide Synthesis Kit (Chiron Technologies Pty. Ltd., Clayton, VIC, Australia) (*46*). The remaining peptides were assembled using an ABI 433A Peptide Synthesizer (Perkin-Elmer Applied Biosystems). Standard solid-phase chemistry based on the Fmoc protecting group was employed (*47*). Peptides were side-chain deprotected and cleaved from the synthesis supports using methods described previously (*48*). All peptides were purified by preparative reversed-phase HPLC or solid-phase extraction (simultaneously synthesized peptides), isolated by lyophilization, and analyzed by analytical HPLC and mass spectrometry (Dynamo DE MALDI-TOF spectrometer; ThermoBioAnalysis Ltd., Hemel Hempstead, Herts, England).

Immobilization of Peptides on Agarose Beads. p21 (141−160) was immobilized on iodoacetyl-cross-linked agarose beads (SulfoLink Kit, Pierce). The SulfoLink support binds specifically to sulfhydryls. There is a 12-atom spacer arm that reduces steric hindrances and makes binding more efficient. For the purpose of immobilization, p21 (141−160) was synthesized with an N-terminal cysteine. The peptide was reduced with 2-mercaptoethanolamine at 37 °C for 1.5 h. Reduced peptide was separated from the reducing reagent using a polyacrylamide gel filtration column (MW exclusion limit of 1800). The peptide was cross-linked to the SulfoLink support at an agarose bead concentration of 1 mg/mL and pH 8.5. The reaction was carried out at room temperature for 45 min. The free iodoacetyl groups, remaining after cross-linking of the peptide, were thiolated with L-cysteine (at room temperature for 45 min). The beads were washed with a 1 M NaCl solution and finally stored in degassed deionized water containing 0.05% NaN_3 at 4 °C.

Fluorimetry. The amount of displaced fluorescein-labeled PCNA was quantified using Biolite F1, a 96-well plate fluorescence reader (BIO-TEK Instruments, Inc.).

Isothermal Titration Calorimetry. Direct measurements of the thermodynamics of peptides binding to PCNA were performed by isothermal titration calorimetry using a VP-ITC system (Heath Scientific Co. Ltd.). PCNA and the peptides with which it was titrated were dissolved and dialyzed extensively against PBS. In a typical experiment, the peptide ligand (200 μM in the syringe) was titrated over 15−30 injections of 5 μL into a 10 μM solution of purified PCNA. The quantity of heat released due to peptide ligand binding to PCNA was measured by integrating the area of each titration peak. Calculation of binding enthalpy, entropy, and stoichiometry from peptide titration data was accomplished using ORIGIN software provided by Heath Scientific Co. Ltd.

SV40 Replication Assay. The SV40 replication assay was performed essentially as originally described by Li and Kelly (*49*), but adapted for 96-well plates. We used Omniplate 96 (Hybaid) 96-well plates with conical bottoms. The final reaction volume in each well was 25 μL, and each well contained 30 mM HEPES (pH 7.5); 7 mM $MgCl_2$; 4 mM ATP; dATP, dCTP, dGTP, and dTTP (100 μM each); CTP, GTP, and UTP (50 μM each); 40 mM phosphocreatine; 0.625 unit of creatine phosphokinase; 50 ng of plasmid DNA; 1 μCi of [α-^{32}P]dCTP; 1 μg of T antigen; and 12 μL of HeLa extract. The cytoplasmic HeLa S100 replication-competent extract was prepared as described previously (*48*). SV40 T antigen was immunopurified from Sf9 cells, infected with baculovirus, containing expression vector for T antigen, as described previously (*50*). A plasmid containing the SV40 origin of replication (pUCHSO) and a control plasmid containing a 4 bp deletion within the SV40 origin of replication (pUC 8-4) were purchased from Cambio and were described previously (*51*, *52*). To assay replication inhibitory activity of peptides, 2 μL of peptide solution was added to each well and the reaction mix was incubated at 37 °C for 4 h. At the end of the incubation period, an aliquot of the reaction mixture was transferred into a 96-well plate with a bounded GF/C filter (Packard) and precipitated with 10% TCA, and the unbound radioactivity was washed out with 5% (w/v) TCA/0.5% (w/v) $Na_4P_2O_7 \cdot 10H_2O$, followed by 95% ethanol. The total counts present in acid-precipitable DNA material were measured by a TopCount-NXT microplate liquid scintillation counter.

RESULTS

Purification and Biochemical Characterization of PCNA. Labeling of Purified PCNA with Fluorescein. Human PCNA, expressed in *E. coli* strain BL21, was purified from the soluble fraction by a three-step procedure, including Q Sepharose (strong anion exchange), SP Sepharose (strong cation exchange), and hydroxyapatite column chromatography (see Materials and Methods for details). Figure 1 shows SDS−PAGE profiles of the pooled PCNA-containing fractions after different chromatographic steps of purification. PCNA is an acidic protein with a low pI (53) and binds very well to anion exchange media. After the first column (Q Sepharose), PCNA is already more than 90% pure (Figure 1A, lane 1). After two additional chromatography steps (SP

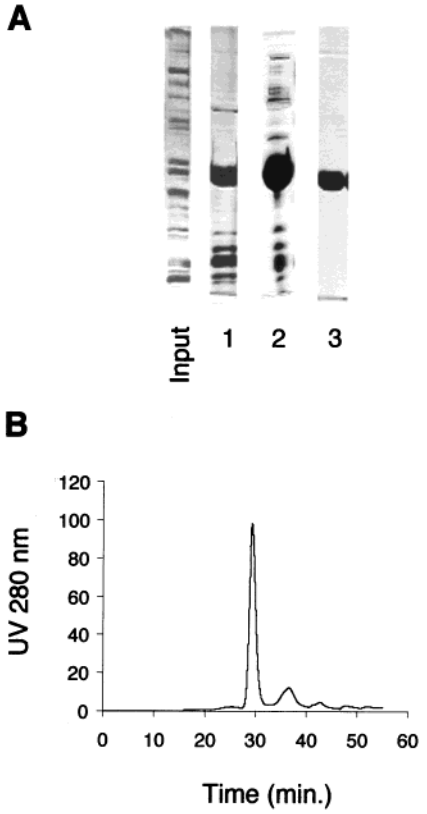

FIGURE 1: Purification and characterization of recombinant human PCNA. (A) SDS−PAGE of PCNA at different steps of purification. Fractions obtained at different steps of purification (1, Q Sepharose; 2, SP Sepharose; and 3, hydroxyapatite) were analyzed by SDS−PAGE and stained with silver (see Materials and Methods for details). (B) Characterization of PCNA trimer by size-exclusion chromatography. A fraction of purified PCNA was analyzed on a Superose-12 column (Pharmacia); the mobile phase was 25 mM Tris-HCl (pH 7.5), 2 mM DTT, 200 mM NaCl, and 10% glycerol, and the flow rate was 0.4 mL/min. The molecular mass of PCNA was determined using gel filtration chromatography standards (Bio-Rad): thyroglobulin, 670 000 Da; bovine γ-globulin, 158 000 Da; chiken ovoalbumin, 44 000 Da; equine myoglobulin, 17 000 Da; and vitamin B_{12}, 1350 Da.

Sepharose and hydroxyapatite), the isolated PCNA was highly pure (more than 99%, Figure 1A, lane 3). Typically, 25 mg of PCNA is produced from 2 L of bacterial culture. The oligomeric state of the purified PCNA was determined by size-exclusion HPLC (Figure 1B). Purified PCNA was very homogeneous, and using a gel filtration calibration kit, the molecular mass of the protein was determined to be 106 000 Da, which corresponds to a trimeric PCNA complex. A similar molecular mass for the PCNA trimer (102 000 Da) was reported by Zhang et al. (*53*). The PCNA trimer is stable both in solution and on DNA (*1*). In solution, the K_d of PCNA dissociation into monomers is 20 nm and the trimer remains stable at 500 mM NaCl (*29*, *54*). The protein was effective in activation of in vitro replication in PCNA-depleted *Xenopus* egg extracts (data not shown).

Purified PCNA was labeled with FLUOS, using a Fluorescein Labeling Kit (Boehringer Mannheim Biochemica; see Materials and Methods for details). The approximate ratio of fluorochrome to protein was determined to be 3:1. Labeled and nonlabeled PCNA were compared on the basis of their SDS−PAGE profiles, oligomeric states (SE HPLC profile), and binding to p21-derived peptides. Both proteins had very similar characteristics (data not shown), which showed that fluorescein labeling did not interfere with the structure and function of PCNA.

"PCNA Competitive Binding" Assay. p21 (141−160), containing N-terminal cysteine, was immobilized on agarose beads at a concentration of 1 mg/mL of slurry (see Materials and Methods for details). The peptide cross-linked with high efficiency, judged by the peptide concentration before and after immobilization. Different amounts of fluorescein-labeled PCNA (PCNA-FLUOS) in PBS buffer were added to p21 (141−160)−agarose beads. PCNA-FLUOS bound strongly to p21 (141−160)−agarose beads; 4 mg of PCNA-FLUOS bound with 100% efficiency to 1 mL of beads (judged by the protein concentration of total and nonbound protein, data not shown). PCNA-FLUOS−p21 (141−160)−agarose beads are very stable and could be stored at 4 °C for a long time (in the presence of an antibacterial agent as NaN_3) with no releasing of the labeled protein in the solution. The minimal amount of labeled protein bound to p21 (141−160)-cross-linked agarose beads providing a good signal-to-noise ratio in competition experiments was determined to be 0.6 mg of PCNA-FLUOS/mL of beads (50% slurry in PBS buffer).

In a typical assay, 20 μL of PCNA-FLUOS−p21 (141−160)−agarose beads (50% slurry) was mixed with 30 μL of different concentrations of a peptide (in PBS buffer). The reaction mixture was incubated for 30 min at room temperature with constant shaking. After that, the beads were separated from the liquid phase by centrifugation (10 000 rpm, microfuge). Ten microliters of the supernatant was added to 30 μL of PBS in a 96-well plate. The fluorescence was measured on a Biolite F1 fluorescence reader: excitation at −460 nm and emission at −520 nm. The fluorescence intensity is proportional to the amount of PCNA-FLOUS released from the p21 (141−160)−agarose beads by the free peptide competitor (Figure 2A).

The PCNA-FLUOS, displaced from the p21 (141−160)−agarose beads, could be visualized by resolving the protein on SDS−PAGE. Figure 2B shows a 12% SDS−PAGE profile of PCNA competed off p21 (141−160)−agarose beads by different concentrations of free p21 (141−160). These data coincide well with the fluorescence measurements. Using QuantiScan, we confirmed the K_i value for the PCNA-FLUOS−p21 (141−160) complex (data not shown).

Increasing the incubation time of the competition reaction above 30 min (1, 2, 6, and 24 h) did not lead to a significant increase in the fluorescence, due to the amount of PCNA-FLUOS competed off by 100 μM free p21 (141−160). This shows that the equilibrium is reached by the 30th min (Figure 2C).

To check the specificity of p21 (141−160) competitive binding, we used as a free ligand a scrambled version of p21 (141−160) (SFRFYRTKSLRMQFKHTDI). Figure 2D shows a SDS−PAGE profile of PCNA, competed off from p21 (141−160)−agarose beads by different concentrations of p21 (141−160) (100, 20, and 1 μM in lanes 1−3, respectively) and its scrambled version (1200, 250, and 50 μM in lanes 4−6, respectively). Even very high concentrations of the scrambled p21 (141−160) (above 1 mM, see lane 4) were not able to compete with the immobilized p21 (141−160) for binding to PCNA.

Structure−Binding Relationship of p21 (141−160). To characterize the structure−binding relationship of p21 (141−

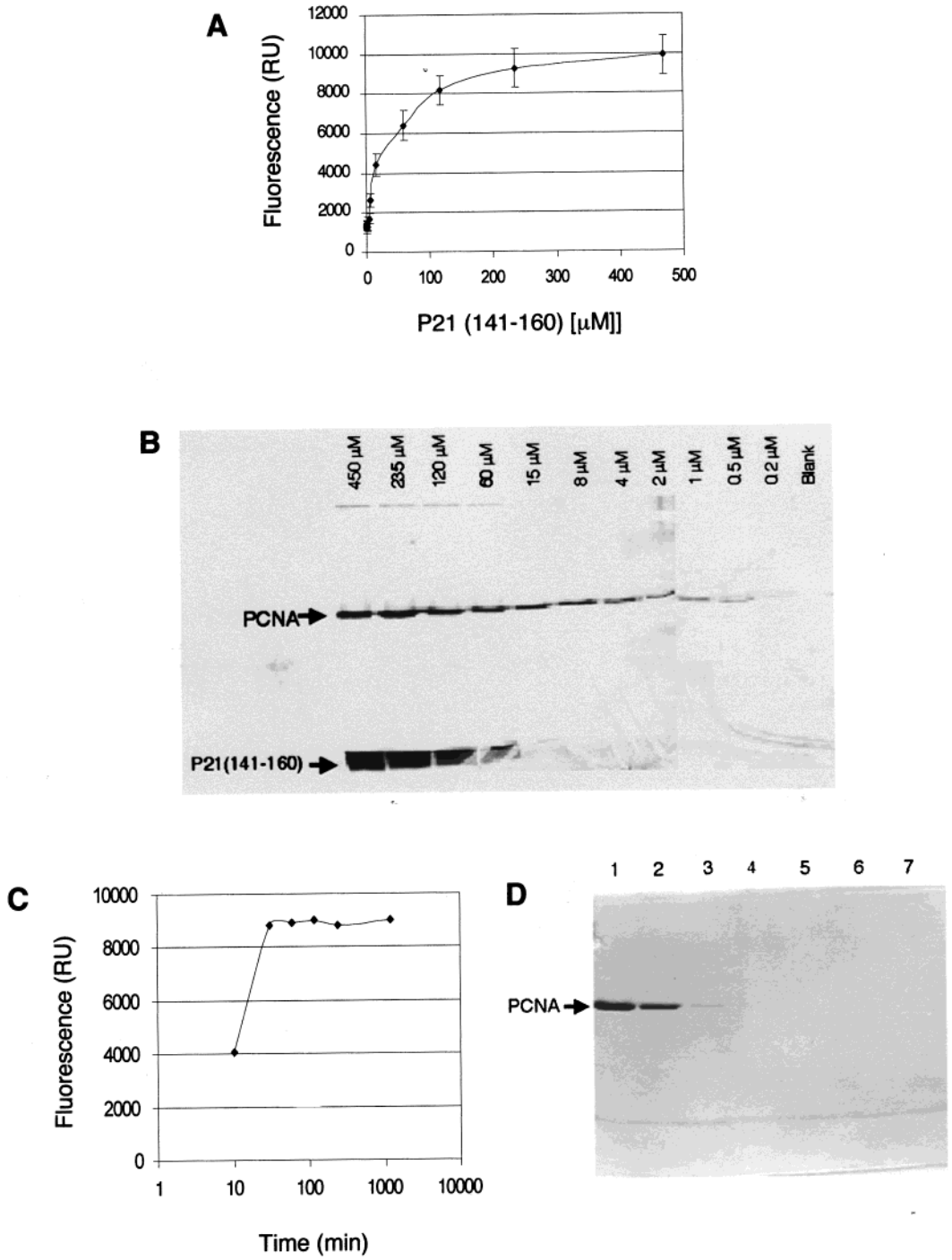

FIGURE 2: Characterization of the PCNA competitive binding assay. (A) Displacement of fluorescein-labeled PCNA from PCNA−p21 (141−160)−agarose beads by free p21 (141−160). Twenty microliters of p21 (141−160)−agarose beads with preimmobilized PCNA (see Materials and Methods for details) was mixed with 30 μL of different concentrations of p21 (141−160). The competitive binding reaction was carried out for 30 min at room temperature with constant shaking. After separation of the beads, the liquid phase was analyzed for fluorescein-labeled PCNA by measuring the fluorescence on a Biolite F1 fluorescence reader: excitation at 460 nm and emission at 520 nm. The data shown are the mean ± SD derived from three different experiments. (B) SDS−PAGE profile of PCNA displaced from PCNA−p21 (141−160)−agarose beads by different concentrations of free p21 (141−160) (the concentrations are indicated above the lanes). The 12% SDS−PAGE gel is stained with silver. Arrowheads indicate the positions of PCNA and p21 (141−160). (C) Time course studies of the PCNA competitive binding reaction. p21 (41−160) (100 μM) was used as a free ligand. The competitive binding reaction was carried out for 15 min, 30 min, 1 h, 2 h, 6 h, and 24 h at room temperature with constant shaking. The competed off FLUOS-PCNA was analyzed by measuring the fluorescence. (D) SDS−PAGE profile of PCNA displaced from PCNA−p21 (141−160)−agarose beads by different concentrations of p21 (141−160) and scrambled p21 (141−160). The 12% SDS−PAGE gel is stained with silver. Arrowheads indicate the positions of PCNA. The concentrations of the free peptides were as follows: lane 1, 100 μM p21 (141−160); lane 2, 20 μM p21 (141−160); lane 3, 1 μM p21 (141−160); lane 4, 1200 μM scrambled p21 (141−160); lane 5, 250 μM scrambled p21 (141−160); lane 6, 50 μM scrambled p21 (141−160); and lane 7, PBS only.

160), a number of truncation and substitution analogues were synthesized (see Table 1) and tested in the PCNA competition assay for their ability to displace PCNA from its complex with immobilized p21 (141−160). Constants of inhibition of different peptides were calculated using GraFit software and represented as a percentage of the constant of inhibition

Table 1: Structure-Binding Relationships of p21 (141−160)[a]

Peptide	Sequence	Ki (% to p21(141-160)
P21 (141-160)	KRRQTSMTDFYHSKRRLIFS	100
P21 (141-160) Arg155,157Ala	KRRQTSMTDFYHSKARAIFS	2265
P21 (141-160) Met147Ala	KRRQTSATDFYHSKRRLIFS	-
P21 (141-160) Asp149Ala	KRRQTSMTAFYHSKRRLIFS	768
P21 (141-158)	KRRQTSMTDFYHSKRRLI	688
P21 (141-156)	KRRQTSMTDFYHSKRR	1519
P21 (141-154)	KRRQTSMTDFYHSK	6660
P21 (141-152)	KRRQTSMTDFYH	3940
P21 (141-150)	KRRQTSMTDF	-
P21 (141-148)	KRRQTSMT	-
P21 (145-156)	TSMTDFYHSKRR	-
P21 (149-160)	DFYHSKRRLIFS	-
P21 (144-151)	QTSMTDFY	-
P21 (147-154)	MTDFYHSK	-
P21 (150-157)	FYHSKRRL	-
P21 (153-160)	SKRRLIFS	-
P21 (153-161)	SKRRLIFSK	-
P21 Consensus motif 1	SAVLQKKITDYFHPKK	42
P21 Consensus motif 2	SAVLQRSIMSFFHPKK	22129
P21 Consensus motif 3	MQRKITDYF	7000

[a] The data in the table represent the relative activity of different truncation and substitution variants of p21 (141−160) in the competitive PCNA binding assay. The K_i (constant of inhibition) values were calculated using GraFit software and normalized to the K_i for p21 (141−160).

of free p21 (141−160). Results are shown in Table 1.

Mutation of Met 147 to Ala abolished the ability of p21 (141−160) to compete with the immobilized wild-type peptide for binding to PCNA. The critical importance of Met 147 for p21−PCNA binding has been shown in several reports (*25*, *26*) as well as clearly demonstrated in the crystal structure of the C-terminal region of $p21^{WAF1/CIP1}$ complexed with human PCNA (*4*). In the structure of the complex, residues ^{146}SMTDFY^{151} adopt a 3_{10}-helical conformation which positions both Met 147 and Tyr 151 of p21 in a hydrophobic cavity under the connector loop of PCNA.

Mutation of Asp 149 to Ala increased significantly (about 8-fold, Table 1) the K_i of p21 (141−160). Similarly, a decrease in binding efficiency and inhibition of in vitro DNA replication of p21 (141−160) D149A were reported by Warbrick et al. (*26*). Asp 149 has been shown in the crystal structure of the p21 (139−160)−PCNA complex to stabilize the 3_{10}-helical configuration (*4*).

The nine C-terminal residues of the peptide (^{152}HSKRRLIFS^{160}) form a β-strand that runs antiparallel to the one formed by the N-terminal portion of the interdomain connector loop (*4*). Arg 155, Arg 156, and Ser 160 are involved in ion-pairing and hydrogen-bonding interactions between the peptide and the interdomain connector loop of PCNA. A small hydrophobic pocket formed at the junction of the connector loop and the underlying β-sheet of the N-terminal domain of PCNA accommodates the side chain of Ile 158 of the peptide (*4*). The importance of the C-terminal residues of p21 (141−160) for inhibition of in vitro replication has been shown by Warbrick et al. (*26*). These authors though could not show a clear correlation between PCNA binding and inhibition of SV40 DNA replication in vitro of p21 (141−160) variants where the C-terminal residues were sequentially changed to alanine. Mutation of Arg 155 and Leu 157 to alanine reduced the affinity of the peptide for PCNA (Table 1). Gradual truncation of the C-terminal residues ^{152}SKRRLIFS^{160} resulted in a gradual increase in K_i (reciprocal to binding affinity), up to 66 times the control level (Table 1). Truncation of Ser 160 and Leu 159 decreased 7-fold the ability of the peptide to compete off PCNA-FLUOS from p21 (141−160)−agarose beads. The smallest peptide, which was still capable of competing with immobilized p21 (141−160) for binding to fluorescently labeled PCNA, was p21 (141−152). Further truncation of the C-terminal residues abolished completely the ability of peptides to compete off the immobilized PCNA-FLUOS.

Truncated variants of p21 (141−160) that did not contain ^{141}KRRQTSMTDFYH^{152} were inactive in the PCNA competitive binding assay (Table 1). As a result of this structure−binding relationship study, we determined a shorter version of p21 (141−160), containing 12 amino acid residues, which retains an ability to compete with the wild-type peptide for binding to PCNA. Truncating the eight C-terminal residues though decreases significantly the PCNA-binding affinity of the peptide, and the K_i for p21 (141−152) is 39 times higher than the one for p21 (141−160) (Table 1).

Rationally Designed Peptides. Due to the fact that our dissection of the p21 (141−160) peptide structure−activity relationship showed that further minimization of this 20-amino acid sequence invariably led to a severe loss in affinity, we turned our attention to conserved PCNA-binding domains in general. It had been demonstrated previously that the following conserved binding motif is present in a subset of proteins, including p21, known to interact with PCNA: QXX(h)XX(a)(a), where X represents any amino acid, (h) indicates moderately hydrophobic residues, and (a) corresponds to aromatic hydrophobic residues (*56*). Considerable variations in the sequences flanking this motif are evident, and the motif itself occurs terminally in at least two cases. Thus, the transposase encoded by the *Pogo* DNA transposon contains the C-terminal sequence QKKITDYF, whereas the N-terminus of DNA ligase I is formed by the sequence QRSIMSFF (*57*). We therefore designed hybrid peptides (consensus motifs 1 and 2; see Table 1) containing either the *Pogo* or DNA ligase I motifs extended with four flanking residues from the *Pogo* (N-terminal) or DNA ligase (C-terminal) sequences (Figure 3). One of these 16-amino acid hybrid compounds (consensus motif 1 peptide) was indeed found to have a better ability to compete off PCNA than the 20-mer p21 (141−160) peptide (Table 1). In contrast, consensus motif 2, containing the DNA ligase I motif (Table 1), exhibited very little ability to compete with p21 (141−160) for binding to PCNA. Consensus motif 3, a 9-mer containing the *Pogo* motif, where one of the Arg residues is replaced with Lys and the flanking regions are missing, was 7-fold less active in a PCNA competitive binding assay than p21 (141−160) (Table 1).

In summary, our initial results with rationally designed peptides suggest that it should be possible to develop lead peptides of suitable size and potency for the purpose of developing drugs exploiting modulation of the p21−PCNA protein−protein interaction.

Characterization of Binding Interactions between PCNA and Different p21 (141−160) Mutants by Isothermal Titration Calorimetry. To validate our results from the PCNA competitive binding assay, we characterized the interactions between PCNA and different p21 (141−160)-derived peptides in solution by isothermal titration calorimetry using VP-ITC system (Heath Scientific Co. Ltd.) (Figure 4). A 200 μM solution of peptide was titrated into a 10 μM solution of PCNA at 30 °C in PBS. The raw data were analyzed by ORIGIN software, and the following parameters were

FIGURE 3: Amino acid sequence alignment of PCNA binding motifs from *Pogo*, DNA ligase I, and p21. Consensus motif peptides were designed as hybrids between *Pogo* and DNA ligase I (highlighted). The consensus motif 1 peptide contains the *Pogo* motif extended to the C-terminus with four flanking residues from DNA ligase. The consensus motif 2 peptide contains the DNA ligase motif extended to the N-terminus with four flanking residues from *Pogo*. The consensus motif 3 peptide contains the *Pogo* motif, where one of the Arg is replaced with Lys (as it is in the DNA ligase motif).

Table 2: Characterization of PCNA Interaction with p21 (141−160), p21 (141−160) Mutants, and the Consensus Motif 1 Peptide by Isothermal Titration Calorimetry

peptide sequence	*N* (stoichiometry)	*K* (affinity constant) (M^{-1})	ΔH (enthalpy) (kcal mol^{-1})	ΔS (entropy) (cal mol^{-1} $°C^{-1}$)
p21 (141−160)	1.0	1.14×10^7	−9758	0.085
p21 (141−160) Met147Ala	–	–	–	–
p21 (141−160) Asp149Ala	0.8	7.82×10^5	−11270	−10.24
consensus motif 1	0.7	1.0×10^7	−9518	0.6083

calculated: affinity constant (*K*), stoichiometry, enthalpy (ΔH), and entropy (ΔS) (Table 2).

The results confirmed the data obtained by the PCNA competition binding assay, namely, that (1) p21 (141−160) Met147Ala does not bind PCNA and (2) p21 (141−160) Asp149Ala has an affinity for PCNA ~10 times lower than that of p21 (141−160). According to the ITC data, consensus motif 1 bound PCNA with the same affinity as p21 (141−160) (Table 2). The K_i for consensus motif 1 determined in a PCNA competitive binding assay, though, was 2-fold lower than the one for p21 (141−160) (Table 1). This difference in the data for the affinity of binding of consensus motif 1 to PCNA could be due to the different types of assay: binding in solution (ITC) and binding to an immobilized target molecule (PCNA competitive binding assay). It is possible as well that consensus motif 1 binds to PCNA with a different stoichiometry, judged by the ITC data (Table 2), which will correspond to two molecules of consensus motif 1 peptide per PCNA trimer. One could speculate that the binding of two molecules of consensus motif 1 peptide to a PCNA trimer alosterically modifies the third binding site and makes it inaccessible for peptide binding. As a result of this model, consensus motif 1 would be able to compete off PCNA at lower concentrations than p21 (141−160). This could explain the higher affinity of consensus motif 1 determined in PCNA competitive binding assay. Further experiments are needed to resolve the matter.

Biological Activity of PCNA-Binding and Mutant Peptides. To examine the effect of different p21-derived and rationally designed PCNA-binding peptides on the PCNA-dependent DNA synthesis, selected peptides were tested for their effect on the replication of SV40 in vitro (Figure 5). Peptides were added to the replication reaction (see Materials and Methods) at a range of concentrations up to 50 μM. At higher concentrations, some of the peptides aggregate and precipitate, and this results in a nonspecific inhibition of the replication reaction. Comparison of the dose dependence curves for the inhibition of replication reveals that p21 (141−160) and consensus motif 1 peptide are potent inhibitors of DNA synthesis. Mutation of Asp 149 to Ala decreased significantly the inhibitory activity of the peptide. In this case, only 40% inhibition was measured at the highest concentration that was used (50 μM). In addition, Met 147 mutation to Ala abolished completely the inhibitory activity of the peptide. The inhibitory activities of the tested peptides show a remarkable correlation with their PCNA binding affinities, confirming the suitability of the PCNA binding assay in the development of PCNA-dependent inhibitors of DNA synthesis.

DISCUSSION

The PCNA−p21 interaction is crucial for the genome integrity and cell cycle control and a very good molecular target for designing therapeutic agents to treat proliferative disorders such as cancer. Our aim was to define a small p21-derived peptide which would be able to mimic the full-length protein activity to inhibit the PCNA function. For this purpose, we needed a quick, quantitative binding assay with reasonable throughput.

The PCNA−p21 interaction is well-characterized, and it has been shown to involve the interdomain connector loop of PCNA and a PCNA binding motif located in the carboxy-terminal part of p21 between residues 144 and 151 (*4*, *24*−*26*, *58*). As the interdomain connector loop of PCNA is a common docking site for other components of the replicative machinery such as DNA pol δ (*33*) and Fen 1 (*26*, *34*), one of the most popular mechanisms of p21 inactivation of PCNA-dependent DNA replication suggested in the literature is competitive binding to PCNA (reviewed in ref *2*).

Using a yeast two-hybrid screen, Warbrick et al. (*26*) determined that a 20-amino acid peptide derived from p21 (^{141}KRRQTSMTDFYHSKRRLIFS^{160}) interacts strongly with purified PCNA, inhibits SV40 DNA replication in vitro, and captures PCNA from whole cell extracts, demonstrating that this peptide retains the binding affinity and biological activity characteristic of the full-length protein. ^{141}KRRQTSMTDFYHSKRRLIFS^{160} was our starting point for further development of p21 peptidomimetic. A complex of p21 (141−160) immobilized on agarose beads with highly purified and homogeneous recombinant PCNA, which was labeled with fluorescein, was used in the PCNA competitive binding assay

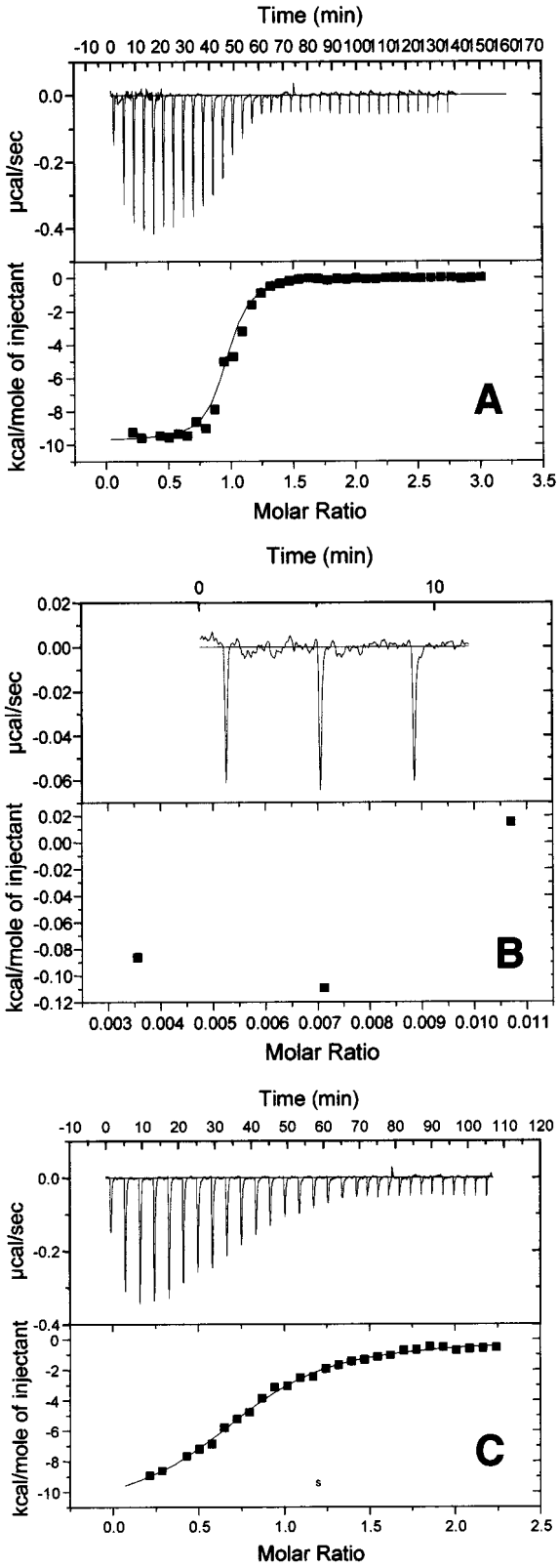

FIGURE 4: Calorimetric titrations of PCNA with (A) p21 (141−160), (B) p21 (141−160) Met147Ala, and (C) p21 (141−160) Asp149Ala. The top part of each panel shows the heat effect associated with the injection of the corresponding peptide (5 μL per injection of a 200 μM solution) into the calorimetric cell containing 10 μM PCNA. The experiments were performed at 30 °C. The bottom parts of panels A and C show the binding isotherms corresponding to the data from the top part of the same panels and the best fitted curve. No curve was fitted from the data in panel C, as no heat effects were detected in this case. Thermodynamic parameters calculated from this experiment are shown in Table 2.

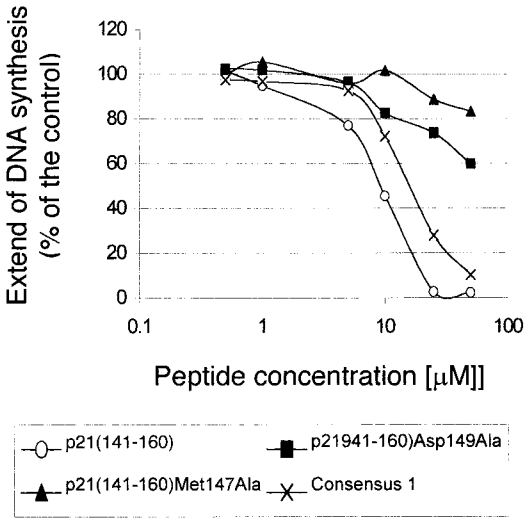

FIGURE 5: Inhibition of in vitro DNA replication by p21-derived and rationally designed PCNA-binding peptides. Peptides were added to an SV40 DNA replication reaction (see Materials and Methods) at the following final concentrations: 0.5, 1, 5, 10, 25, and 50 μM. Incorporation of [α-^{32}P]dCTP was assessed by TCA precipitation and scintillation counting. Background incorporation of radioactivity in a sample with a mutant plasmid (containing a 4 bp deletion within the SV40 origin of replication) and no large T antigen added were subtracted from all measurements. The extent of DNA synthesis in all samples is expressed as a percentage of the control sample where the equivalent amount of buffer only was added. All peptide concentrations were tested in triplicate. CV values in all experiments were less than 10.

reported here. p21 (141−160) derivatives were tested for their abilities to modulate the ^{141}KRRQTSMTDFYHSKRRLIFS^{160}−PCNA interaction, and inhibition constants (K_i) were calculated.

The crystal structure of a similar peptide from the C-terminus of p21, e.g., p21 (139−160) complexed with PCNA, stipulates that both the C- and N-terminus of the peptide are important for the interaction (*4*). It also suggests that some residues such as Met 147, Asp 149, Arg 155, and Ser 160 are critical due to their involvement in ion-pairing, hydrogen-bonding, and hydrophobic interactions. To check these predictions, Met 147 and Asp 149 were substituted for Ala and the mutant peptides tested in the PCNA competitive binding assay. p21 (141−160) Met147Ala did not compete for binding to PCNA, while p21 (141−160) Asp149Ala had activity reduced approximately 8-fold compared to that of the original peptide. Mutations and truncations in the C-terminus of p21 (141−160) inhibited significantly (15−66-fold), while N-terminal truncations abolished completely, the ability of the peptide to compete for PCNA binding.

The smallest peptide, which was still capable of competing with immobilized p21 (141−160) for binding to FLUOS-labeled PCNA, was p21 (141−152) containing four basic residues (^{141}KRR^{143} and ^{152}H) and the PCNA binding region (QTSMTDFY) (*25*, *26*), where Met 147 and Phe 150 are critical and Asn 144, Asp 149, and Tyr 151 are important residues. The ^{144}QTSMTDFY^{151} peptide alone, though, was not active in the PCNA competitive binding assay (Table 1), which emphasizes the importance of the basic regions flanking the binding motif. The residues of the N-terminal portion of the peptide interact with the C-terminus of PCNA molecule via ion pairing, but in the crystal structure of the

PCNA−p21 (139−160) complex, they are poorly ordered (*4*). Studying the structure−activity relationships of p21 (141−160), Warbrick et al. (*26*) did not detect a significant change in the PCNA binding when the N-terminal basic residues (^{141}KRR^{144}) were altered to alanine, though these changes resulted in a decrease in the extent of inhibition of SV40 DNA replication in vitro induced by the peptide.

The interactions between PCNA and p21 (141−160), p21 (141−160) M147A, and p21 (141−160) D149A were characterized by another independent method, isothermal titration calorimetry (ITC). The affinity constant for the interaction between p21 (141−160) peptide and PCNA has been determined to be 1.14×10^7 M^{-1}, corresponding to a K_d of 87.7 nM, which is approximately 6−8 times higher than the value determined for the full-length p21 (K_d = 10−15 nM) and in a range very similar to the one determined for Fen 1 (K_d = 60 nM) (*23*, *34*, *58*). The data obtained by ITC confirm previous reports that the stoichiometry of the p21 (141−160)−PCNA interaction is 1:1; e.g., a trimeric PCNA binds three peptides (*4*). p21 (141−160) M147A did not bind to PCNA as assessed by ITC, and the K_d value for the p21 (141−160) D149A−PCNA interaction was about 10 times higher that the one for the wild-type peptide. The ITC data coincide well with the PCNA competitive binding data and the crystal structure of PCNA and the C-terminal domain of p21 (*4*). The binding affinities of p21 (141−160), p21 (141−160) M147A, and p21 (141−160) D149A correlated well with the abilities of these peptides to inhibit in vitro SV40 DNA replication.

Dissection of the p21 (141−160) peptide structure−activity relationship showed that further minimization of this 20-amino acid sequence invariably led to a loss of binding affinity. On the basis of conserved PCNA-binding motifs from *Pogo* transpoase and DNA ligase I, we have designed consensus motif peptides and tested their abilities to compete with p21 (141−160) for binding to PCNA.

As a result, a 16-residue peptide, containing the sequence QKKITDYF (derived from *Pogo* transposase), was shown to have a high binding affinity for PCNA. These results were confirmed by ITC data. The affinity of the consensus motif 1 peptide for PCNA is similar to that of the p21 (141−160) peptide, but its stoichiometry and PCNA binding site need to be further clarified. Both peptides were able to inhibit SV40 DNA replication in vitro to a similar extent, though the consensus motif 1 peptide inhibitory effect was reached at slightly higher concentrations than p21 (141−160). In addition to its PCNA binding properties, p21 (141−160) contains a cyclin binding motif "LIF", and it has been shown to bind and inhibit the G1 CDK−cyclin complexes (*36*). Consensus motif 1 peptide does not contain the cyclin binding motif and is not able to inhibit CDK−cyclin kinase activity in vitro (paper in preparation). To clarify the effect of CDK inhibition on SV40 DNA replication, we used Roscovitine, a specific CDK−kinase inhibitor (*60*). Roscovitine did not affect significantly SV40 DNA replication in vitro at concentrations up to 50 μM (sufficient to inhibit completely CDK activity in vitro). The slightly higher inhibitory activity of p21 (141−160) in the SV40 DNA replication assay in comparison to that of the consensus motif 1 peptide might be due to the larger size of the former, which could cause additional steric interference with components of the replication machinery. The ability to inhibit DNA replication without inhibition of CDKs makes the consensus motif I peptide a good tool for studying the cellular effects of a specific inhibition of PCNA-dependent DNA replication.

The results in this report have implications for drug discovery using peptide epitope strategies. Peptides targeting a distinct domain of PCNA can prove to be useful tools for dissecting different PCNA-dependent biological processes such as eukaryotic, prokaryotic, and viral replication and DNA repair.

REFERENCES

1. Kelman, Z. (1997) *Oncogene 14*, 629−640.
2. Cox, L. S. (1997) *Trends Cell Biol. 7*, 493−497.
3. Krishna, T. S., Kong, X. P., Gary, S., Burgers, P. M., and Kuriyan, J. (1994) *Cell 79*, 1233−1243.
4. Gulbis, J. M., Kelman, Z., Hurwitz, J., O'Donnel, M., and Kurian, J. (1996) *Cell 87*, 297−306.
5. Burgers, P. M. (1991) *J. Biol. Chem. 266*, 22698−22706.
6. Prelich, G., Tan, C. K., Kostura, M., Mathews, M. B., So, A. G., Downey, K. M., and Stillman, B. (1987) *Nature 326*, 517−520.
7. Bravo, R., Frank, R., Blundell, P. A., and Macdonald-Bravo, H. (1987) *Nature 326*, 515−517.
8. Maga, G., and Hubscher, U. (1995) *Biochemistry 34*, 891−901.
9. Li, X., Li, J., Harrington, J., Lieber, M. R., and Burgers, P. M. (1995) *J. Biol. Chem. 270*, 22109−22112.
10. Shivji, M. K. K., Kenny, M. K., and Wood, R. D. (1992) *Cell 69*, 367−374.
11. Umar, A., Buermeyer, A. B., Simon, J. A., Thomas, D. C., Clark, A. B., Liskay, R. M., and Kunkel, T. A. (1996) *Cell 87*, 65−73.
12. Matsuoka, S., Yamaguchi, M., and Matsukage, A. (1994) *J. Biol. Chem. 269*, 11030−11036.
13. Smith, M. L., Chen, I. T., Zhan, Q., Bae, I., Chen, C. Y., Gilmer, T. M., Kastan, M. B., O'Connor, P. M., and Fornace, A. J., Jr. (1994) *Science 266*, 1376−1379.
14. Hall, P. A., Kearsey, J. M., Coates, P. J., Norman, D. G., Warbrick, E., and Cox, L. S. (1995) *Oncogene 10*, 2427−2433.
15. Vairapandi, M., Balliet, A. G., Fornace, A. J., Jr., Hoffman, B., and Leibermann, D. A. (1996) *Oncogene 12*, 2579−2594.
16. Prosperi, E. (1997) *Prog. Cell Cycle Res. 3*, 193−210.
17. El-Deiry, W. S., Tokino, T., Velculescu, V. E., Levy, D. B., Parsons, R., and Trent, J. M. (1993) *Cell 75*, 817−825.
18. Morgan, D. O. (1997) *Annu. Rev. Cell Dev. Biol. 13*, 261−291.
19. Xiong, Y., Hannon, G. J., Zhang, H., Casso, D., Kobayashi, R., and Beach, D. (1993) *Nature 366*, 701−704.
20. Harper, J. W., Adami, G. R., Wei, N., Keyomarsi, K., and Elledge S. J. (1993) *Cell 75*, 805−816.
21. Zhang, H., Xiong, Y., and Beach, D. (1993) *Mol. Biol. Cell 4*, 897−906.
22. Gu, Y., Turck, C. W., and Morgan, D. O. (1993) *Nature 366*, 707−710.
23. Chen, J., Peters, R., Saha, P., Lee, P., Theodoras, A., Pagano, M., Wagner, G. J., and Dutta, A. (1996) *Nucleic Acid Res. 24*, 1727−1733.
24. Goubin, F., and Ducommun, B. (1995) *Oncogene 10*, 2281−2287.
25. Nakanishi, M., Robetorye, R. S., Periera-Smith, O. M., and Smith, J. R. (1995) *J. Biol. Chem. 21*, 17060−17063.
26. Warbrick, E., Lane, D. P., Glover, D. M., and Cox, L. S. (1995) *Curr. Biol. 5*, 275−282.
27. Flores-Rozas, H., Kelman, Z., Dean, F. B., Pan, Z. Q., Harper, J. W., Elledge, S. J., O'Donnell, M., and Hurwitz, J. (1994) *Proc. Natl. Acad. Sci. U.S.A. 30*, 8655−8659.
28. Li, R., Waga, S., Hannon, G. J., Beach, D., and Stillman, B. (1994) *Nature 371*, 534−537.
29. Podust, V. N., Podust, L. M., Muller, F., and Hubscher, U. (1995) *Biochemistry 34*, 5003−5010.

30. Waga, S., Hannon, G. J., Beach, D., and Stillman, B. (1994) *Nature 371*, 534−537.
31. Li, J. J., Hannon, G. J., Beach, D., and Stillman, B. (1996) *Curr. Biol. 6*, 189−199.
32. Shivji, M. K., Ferrari, E., Ball, K., Hubscher, U., and Wood, R. D. (1998) *Oncogene 17*, 2827−2838.
33. Zhang, P., Sun, Y., Hsu, H., Zhang, L., Zhang, Y., and Lee, M. Y. (1998) *J. Biol. Chem. 273*, 713−719.
34. Warbrick, E., Lane, D. P., Glover, D. M., and Cox, L. S. (1997) *Oncogene 14*, 2313−2321.
35. Cayrol, C., Knibehler, M., and Ducommun, B. (1998) *Oncogene 16*, 311−320.
36. Ball, K. L., Lain, S., Fåhraeus, R., Smythe, C., and Lane, D. P. (1996) *Curr. Biol. 7*, 71−80.
37. Bonfanti, M., Taverna, S., Salmona, M., D'Incalci, M., and Broggini, M. (1997) *Cancer Res. 57*, 1442−1446.
38. Fåhraeus, R., Paramio, J. M., Ball, K. L., Lain, S., and Lane, D. P. (1996) *Curr. Biol. 6*, 84−91.
39. Gius, D. R., Ezhevsky, S. A., Becker-Hapak, M., Nagahara, H., Wei, M. C., and Dowdy, S. F. (1999) *Cancer Res. 59*, 2577−2580.
40. Hupp, T. R., Sparks, A., and Lane, D. P. (1995) *Cell 83*, 337−345.
41. Picksley, S. M., Vojtesek, B., Sparks, A., and Lane, D. P. (1994) *Oncogene 9*, 2523−2529.
42. Bottger, A., Bottger, V., Sparks, A., Liu, W. L., Howard, S. F., and Lane, D. P. (1997) *Curr. Biol. 1*, 860−869.
43. Sekiguchi, T., and Hunter, T. (1998) *Oncogene 22*, 369−380.
44. Niculescu, A. B., III, Chen, X., Smeets, M., Hendst, L., Prives, C., and Reed, S. I. (1998) *Mol. Cell. Biol. 18*, 629−643.
45. Laemmli, U. K. (1970) *Nature 227*, 680−685.
46. Valerio, R. M., Bray, A. M., Campbell, M., Dipasquale, A., Margellis, C., Rodda, S. J., Geysen, H. M., and Maeji, N. J. (1993) *Int. J. Pept. Protein Res. 42*, 1−9.
47. Fields, G. B., and Noble, R. L. (1990) *Int. J. Pept. Protein Res. 35*, 161−214.
48. King, D. S., Fields, C. G., and Fields, G. B. (1990*) Int. J. Pept. Protein Res. 36*, 255−266.
49. Li, J. J., and Kelly, T. J. (1984) *Proc. Natl. Acad. Sci. U.S.A. 81*, 6973−6977.
50. Kernohan, N. M., Hupp, T. R., and Lane, D. P. (1996) *J. Biol. Chem. 271*, 4954−4960.
51. Li, J. J., Peden, K. W. C., Dixon, R. A. F., and Kelly, T. J. (1986) *Mol. Cell. Biol. 6*, 1117−1128.
52. Wold, M. S., Li, J. J., and Kelly, T. J. (1987) *Proc. Natl. Acad. Sci. U.S.A. 84*, 3643−3647.
53. Kelman, Z., and O'Donnell, M. (1995) *Nucleic Acid Res. 23*, 3613−3620.
54. Zhang, P., Zhang, S.-J., Zhang, Z., Woessner, J. F., and Lee, M. (1995) *Biochemistry 34*, 10703−10712.
55. Yao, N., Turner, J., Kelman, Z., Stukenberg, P. T., Dean, F., Shechter, D., Pan, Z.-Q., Hurwitz, J., and O'Donnell, M. (1996) *Genes Cell 1*, 101−113.
56. Warbrick, E., Heatherington, W., Lane, D. P., and Glover, D. M. (1998) *Nucleic Acids Res. 26*, 3925−3932.
57. Montecucco, A., Rossi, R., Levin, D. S., Gary, R., Park, M. S., Motycka, T. A., Ciarrocchi, G., Villa, A., Biamonti, G., and Tomkinson, A. E. (1998) *EMBO J. 7*, 3786−3795.
58. Chen, J., Jackson, P. K., Kirschner, M. W., and Dutta, A. (1995) *Nature 374*, 386−388.
59. Knibiehler, M., Goubin, F., Escalas, N., Jonsson, Z. O., Mazarguil, H., Hubscher, U., and Ducommun, B. (1996) *FEBS Lett. 391*, 66−70.
60. De Azevedo, W. F., Leclerc, S., Meijer, L., Havlicek, L., Strand, M., and Kim, S.-H. (1997) *Eur. J. Biochem. 243*, 518−526.

BI992498R